OPTIMIZATION OF THE RESPONSE MATRIX MEASUREMENT APPLICATION IN PYAPAS

Y. Zhao*, H. Ji, D. Ji, Y. Wei, H. Xu, Institute of High Energy Physics, Beijing, China

Abstract

Measurement of the response matrix serves as the foundation for orbit correction and optics correction. To obtain more accurate response matrix (RM) data while minimizing the measurement time in storage ring of High Energy Photon Source (HEPS), we have meticulously optimized parameters such as the number of data points collected by Beam Position Monitors (BPMs) and the waiting time. Additionally, due to the long overall measurement duration for the entire ring, factors including orbit drift and hysteresis effects during the process can introduce deviations to the measurement results. Therefore, we integrate RM measurement with orbit correction and radio frequency (RF) adjustment to further ensure the consistency of the beam state throughout the entire measurement process. This paper will elaborate on the relevant work in detail.

INTRODUCTION

HEPS is a fourth-generation synchrotron radiation light source [1]. It comprises a 500 MeV S-band linac, a 454 m full-energy booster synchrotron, a 1.36 km storage ring, and three beam transport lines. Designed as a high-energy DLSR operating at 6 GeV, HEPS utilizes a modified hybrid seven-bend achromat (7BA) lattice to achieve an ultra-low natural emittance of approximately 35 pm·rad. With rigorous on-site testing on October 29, 2025, it is confirmed that all Key Performance Parameters were (KPPs) met or exceeded specifications, validating the robustness of the accelerator design and the precision of its engineering. HEPS is currently in the trial operation phase.

Pyapas (Python-based Accelerator Physics Application Set) is a pure Python framework developed at IHEP for accelerator online commissioning and simulation [2]. The program architecture is shown in Fig. 1. It adopts a modular and model-based design, built on physical quantities rather than raw device values. Pyapas provides integrated GUI tools for orbit correction, response matrix measurement, optics analysis, and machine parameter control. It has been successfully deployed at HEPS and extended to other accelerator projects.

The response matrix serves as the fundamental basis for orbit correction, optics correction, and orbit feedback. Accordingly, we developed an upper-level application based on Pyapas, which integrates functions of response matrix measurement and orbit correction. This application has been successfully implemented in the beam commissioning of the Linac [3] and booster [4] of HEPS. As a diffraction-limited storage ring (DLSR), the HEPS storage ring comprises 575 beam-position monitors (BPMs) and 1152 corrector magnets, leading to considerable time consumption for full-ring response matrix measurement. Slow orbit drifts during measurement are non-negligible. In addition, closed-orbit distortions accumulate throughout the measurement due to hysteresis effects and other factors, degrading the measurement precision of the response matrix. In preliminary work, we systematically optimized measurement parameters, including program logic, data acquisition counts per BPM, and hardware settling waiting time, aiming to minimize measurement duration while ensuring measurement validity. Under the current network environment of HEPS, the full-ring response matrix measurement takes 3–4.5 hours. To further improve measurement precision, we incorporated orbit correction and RF frequency correction into the response matrix measurement procedure.

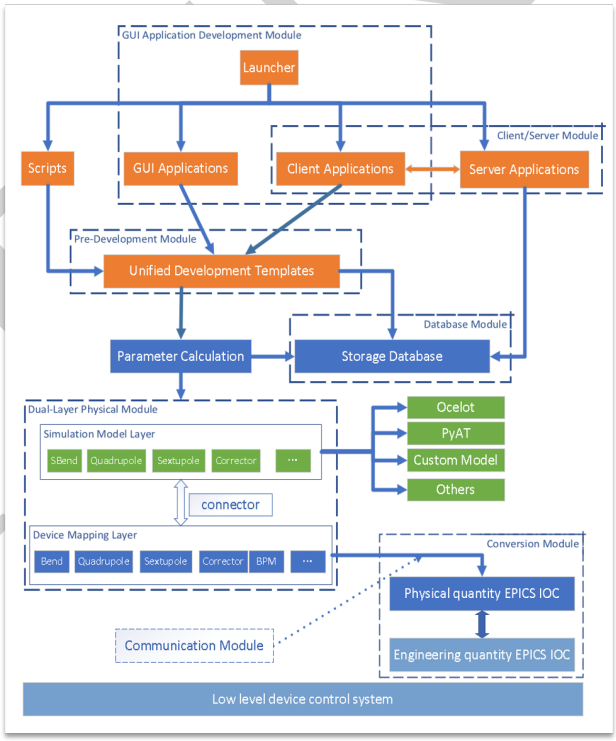

Figure 1: Architecture of Pyapas.

EXTENSION OF RESPONSE MATRIX MEASUREMENT PROCEDURE

Response matrix measurement in a large storage ring requires sequentially exciting individual correctors and reading BPM responses. For HEPS, the full-ring measurement involves a large number of correctors and BPMs, leading to long measurement durations. During this process, slow orbit drift, power supply hysteresis, and RF frequency variations

* zhaoyl@ihep.ac.cn

introduce cumulative orbit distortion, which biases the linear response and degrades matrix accuracy. To address this, we extended the measurement procedure with automatic orbit correction and RF frequency correction. The interface of the application is shown in Fig. 2.

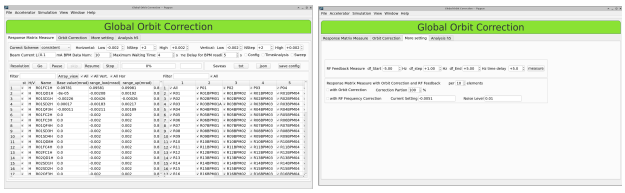

Figure 2: Layout of response matrix measure application.

Automatic RF Frequency Correction

Slow orbit drift induces global energy shifts and dispersion-related orbit changes, which accumulate during matrix measurement. We implemented an automatic frequency correction module that adjusts the RF frequency periodically during measurement, maintaining the beam energy close to the reference value.

The performance of the correction is summarized in Table 1. With RF correction, the maximum horizontal orbit variation (Xmax) reaches 56.1 µm, while without correction it increases to 116.1 µm; however, the RMS variation (XRms) is significantly reduced in many cases, and the vertical maximum variation (Ymax) is suppressed from 35.2 µm to 39.4 µm. The correction effectively stabilizes the beam orbit during long measurement sequences, reducing the systematic bias introduced by slow energy drift.

Automatic Orbit Correction

Local orbit distortion induced by corrector excitation can propagate and accumulate. To reduce the impact of orbit distortion on response matrix accuracy, we integrated automatic global orbit correction into the matrix measurement procedure, which is applied automatically after completing scans of a certain number of correctors. Specifically, orbit correction is executed after measuring the response of every 10 correctors. Although the principle of orbit correction is relatively straightforward, diverse practical scenarios need to be addressed. To guarantee program reliability, we conducted a dedicated analysis on the selection of the singular value decomposition (SVD) mode number for orbit correction. First, the R01SD1H corrector was used to perturb the full-ring orbit, inducing an overall orbit distortion of approximately 20 µm, which is comparable to the distortion introduced by measuring one type of corrector during response matrix measurement, as illustrated in Fig. 3.

Subsequently, orbit correction was performed using 8 correctors and 24 correctors, respectively. The residual closed orbit and corrector variations caused by different singular value settings were investigated under the two configurations. The orbit distortions are shown in Fig. 4 and Fig. 5, while the corrector variations are summarized in Table 2 and Table 3.

The results indicate that, when using 8 correctors, both the corrector strength variations and residual closed orbit remain

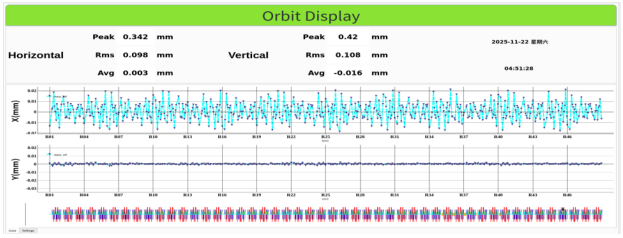

Figure 3: The orbit varation induced by R01SD1H with respect to the reference orbit.

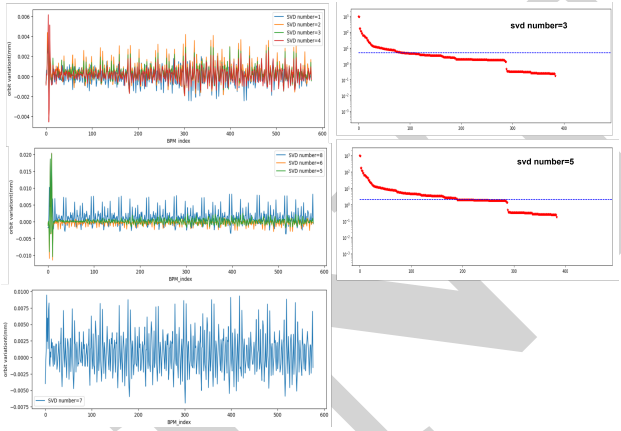

Figure 4: Orbit residuals under different SVD mode configurations with 8 correctors.

small(<6 µm) if the number of SVD modes is no more than 4; however, large local orbit distortion or an overall amplified orbit deviation tends to occur when the SVD mode number is greater than or equal to 5. In contrast, when using 24 correctors, the residual closed orbit and corrector strength variations show little dependence on the choice of SVD mode number. Therefore, for automatic orbit correction, it is recommended to use as many correctors as possible. If only a small number of correctors are available, the number of SVD modes should be kept as low as possible, preferably no more than half of the total number of modes.

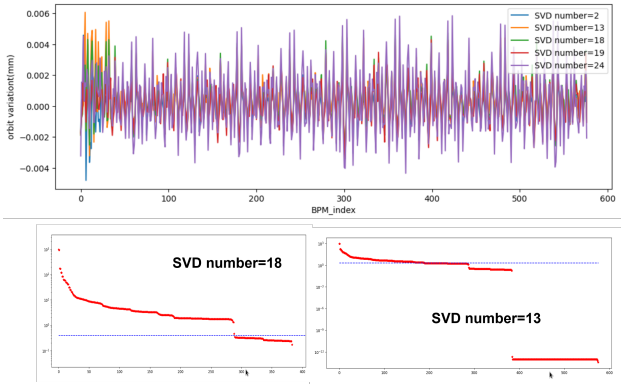

Figure 5: Orbit residuals under different SVD mode configurations with 24 correctors.

Table 1: Accumulated Orbit Statistics with and Without RF Correction (units: μm, tunes are dimensionless)

Condition	Kind	tuneX	tuneY	variation of statistic value of orbit						Statistic of orbit variation			
				Xmax	Ymax	XRms	Yrms	AvgX	AvgY	Xmax	Ymax	XRms	Yrms
without rf correction	FC1/4H	-0.01	-0.0024	-4.6	-5.4	0.4	-0.4	0.2	-0.1	25.2	7.9	7.1	2.5
	SD1/4H	-0.0108	-0.0031	-4.5	-3.2	0.4	0.1	0.6	-0.3	23.8	8.3	6.7	2.1
	FC2/3H	-0.0106	-0.0041	-14.3	-3.6	2.1	0.3	2.4	-0.4	35.4	12.3	9.9	3.2
	SD2/3H	-0.0082	-0.0028	-18.7	-3.7	2.7	0.6	3.7	-0.5	42.8	13.9	12.1	3.5
	FC1/4V	-0.0084	-0.0044	-9.1	-5.1	5.2	0.8	7.1	-0.8	56.7	20.7	14.4	5.4
	SD1/4V	-0.0053	-0.0016	9.4	-7.4	8.5	0.4	11.3	0.1	73.6	19.1	18.2	5.6
	FC2/3V	-0.0035	0.0019	32.1	-5.5	12.3	0.5	15.4	-0.3	98.9	30.1	23.9	7.7
	SD2/3V	-0.003	0.0014	56.2	-5.9	16.5	1.5	19.6	-1.2	116.1	39.4	29.7	10.3
with rf correction	FC1/4H	–	–	-2.6	-12.5	3.0	-1.7	0.5	0.2	33.0	12.9	11.5	4.0
	SD1/4H	-0.0024	-0.0029	-5.6	-10.1	2.6	-1.2	0.2	0.1	32.9	12.0	12.3	3.8
	FC2/3H	-0.0034	-0.0039	-12.6	-11.6	2.0	-1.1	-1.0	0.1	44.8	16.8	16.6	4.9
	SD2/3H	-0.0004	-0.0029	-8.7	-12.0	2.4	-1.1	-1.0	0.2	46.7	18.3	17.9	5.4
	FC1/4V	-0.0004	-0.0049	-8.1	-17.5	2.5	-1.5	-0.9	-0.1	48.9	23.2	18.8	6.7
	SD1/4V	-0.0014	-0.0039	-8.3	-18.6	2.6	-1.5	-0.6	0.5	46.4	21.9	18.7	6.8
	FC2/3V	-0.0004	-0.0039	-11.6	-19.0	2.6	-2.0	-0.5	0.2	51.3	30.0	21.2	8.9
	SD2/3V	-0.0044	-0.0039	-15.5	-18.8	2.6	-1.6	-0.6	-0.4	56.1	35.2	21.8	10.1

Table 2: Corrector Angle Variations under Different SVD Mode Numbers with 8 Correctors (unit: μrad)

Corrector	base value	delta angle under different SVD mode number						
	(μrad)	1	3	4	5	6	7	8
R01FC1H	23.72	0.08	-0.19	-0.17	-0.53	-2.99	0.12	5.17
R01SD1H	-9.40	-0.30	-0.44	0.00	-1.07	3.13	-0.34	-28.92
R01SD2H	1.68	-0.30	-0.32	0.05	-1.00	1.24	-0.29	37.75
R01FC2H	34.61	0.26	0.27	0.19	0.51	7.28	0.26	15.06
R01FC3H	4.72	-0.33	-0.34	-0.38	1.55	8.26	-0.30	16.03
R01SD3H	23.40	0.30	0.38	0.74	0.39	2.33	0.34	42.95
R01SD4H	13.25	0.41	0.48	0.88	0.71	4.55	0.39	-30.53
R01FC4H	54.34	-0.01	0.27	0.21	-0.21	-2.63	0.05	6.58

Table 3: Corrector Angle Variations under Different SVD Numbers with 24 Correctors (unit: μrad)

Corrector	base value	delta angle under different SVD mode number				
	(μrad)	2	13	18	19	24
R01FC1H	23.72	0.08	-1.22	-0.82	-0.22	1.08
R01SD1H	-9.40	-0.20	-0.20	-1.10	-2.60	–
R01SD2H	1.70	-0.20	-0.40	-0.90	-0.20	–
R01FC2H	34.61	0.19	2.89	0.89	0.09	1.99
R01FC3H	4.72	-0.22	1.98	1.48	0.18	2.08
R01SD3H	23.40	0.20	0.80	0.80	1.30	–
R01SD4H	13.25	0.25	1.45	1.15	-0.95	–
R01FC4H	54.34	0.16	0.06	0.16	0.46	0.76
R02FC1H	-17.60	-0.30	-0.10	0.00	0.20	0.90
R02SD1H	4.40	0.10	1.70	1.10	-0.70	–
R02SD2H	-12.50	0.20	1.10	0.70	0.90	–
R02FC2H	14.80	-0.20	2.50	1.60	0.50	2.00
R02FC3H	17.40	0.00	2.10	1.70	0.70	1.90
R02SD3H	-14.80	-0.10	1.00	0.70	1.30	–
R01SD4H	-3.20	-0.20	1.80	1.30	-0.80	–
R02FC4H	47.70	-0.10	0.40	0.10	0.30	0.90
R03FC1H	-24.30	0.20	0.70	0.20	0.30	0.60
R03SD1H	-9.10	0.00	1.40	1.00	-0.80	–
R03SD2H	-7.70	-0.10	0.80	0.50	1.20	–
R03FC2H	0.20	0.10	1.90	1.60	0.60	1.80
R03FC3H	14.60	0.00	1.80	1.50	0.40	1.80
R03SD3H	-19.80	0.00	0.70	0.40	0.90	–
R03SD4H	-16.20	0.00	1.10	0.80	-0.60	–
R03FC4H	0.20	-0.60	-0.50	0.10	0.80	–

Orbit correction functionality integrated into the response matrix measurement procedure has been developed and validated via preliminary experiments. Nevertheless, this feature is not yet enabled for ongoing measurements due to insufficient program testing.

SUMMARY

We optimized the response matrix measurement procedure in the Pyapas framework for HEPS. To mitigate orbit drift and hysteresis effects during long measurements, we implemented automatic RF frequency correction and automatic orbit correction. The RF correction reduces the vertical orbit variation significantly, and the RMS values are improved in most cases. Orbit correction with optimized SVD settings suppresses local distortion and ensures stable beam conditions. The extended procedure significantly improves measurement accuracy and reliability, supporting high-precision commissioning at HEPS.

REFERENCES

[1] Y. Jiao *et al.*, "Status of HEPS Lattice Design and Physics Studies", in *Proc. SAP'17*, Jishou, China, Aug. 2017, pp. 7–9. doi:10.18429/JACoW-SAP2017-MOBH2

[2] X. H. Lu *et al.*, "Pyapas: A New Framework for High Level Application Development at HEPS", in *Proc. 67th ICFA Adv. Beam Dyn. Workshop Future Light Sources (FLS'23)*, Luzern, Switzerland, Aug.–Sep. 2023, pp. 77–79. doi:10.18429/JACoW-FLS2023-TU3B3

[3] Y.-L. Zhao *et al.*, "The high level applications for the HEPS Linac", *J. Instrum.*, vol. 18, p. P06014, Jun. 2023. doi:10.1088/1748-0221/18/06/P06014

[4] Y. Peng *et al.*, "Development of high-level applications for High Energy Photon Source booster", *J. Instrum.*, vol. 19, p. P08013, Aug. 2024. doi:10.1088/1748-0221/19/08/P08013